Square planar Pd(II)/oximate complexes as 'metalloligands' for the directional assembly of 4f-metal ions: A new family of {Ln_2Pd} (Ln = lanthanide) clusters exhibiting slow magnetization relaxation

Konstantinos N. Pantelis,[a] Catherine P. Raptopoulou,[b] Vassilis Psycharis,*[,b] Jinkui Tang,[c] and Theocharis C. Stamatatos*[,a,d]

[a] Department of Chemistry, University of Patras, 26504 Patras, Greece. E-mail: thstama@upatras.gr; Tel: +30 2610 996730.

[b] Institute of Nanoscience and Nanotechnology, NCSR "Demokritos", Aghia Paraskevi Attikis 15310, Greece. E-mail: v.psycharis@inn.demokritos.gr; Tel.: +30-2106503346.

[c] State Key Laboratory of Rare Earth Resource Utilization, Changchun Institute of Applied Chemistry, Chinese Academy of Sciences, Changchun 130022, P. R. China.

[d] Institute of Chemical Engineering Sciences, Foundation for Research and Technology – Hellas (FORTH/ICE – HT), Platani, P.O. Box 1414, 26504, Patras, Greece.

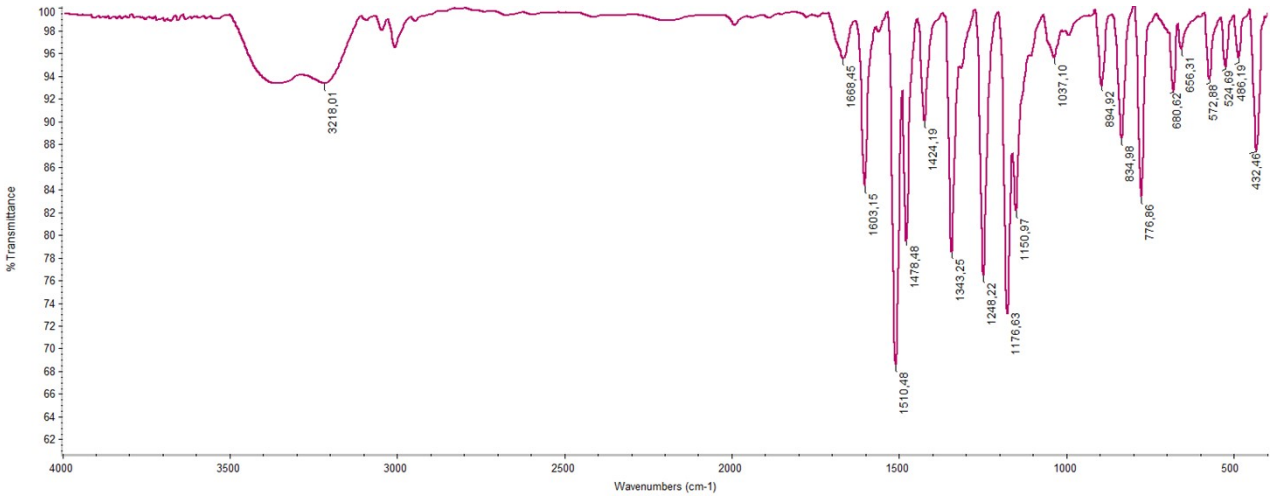

Figure S1. FT-IR spectrum of the 'metalloligand' $[Pd(pao)_2]$ (**1**).

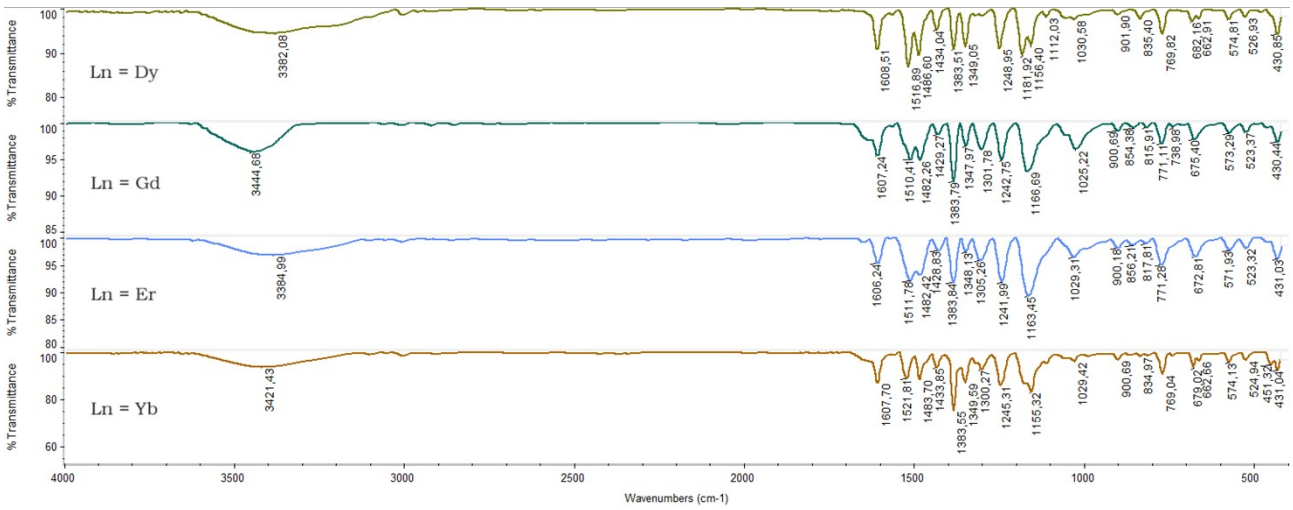

Figure S2. FT-IR spectra of $[Ln_2Pd(pao)_2(NO_3)_6(MeOH)_2(H_2O)_2]\cdot[Pd(pao)_2]_4$ complexes, where Ln^{III} = Dy (**2**), Gd (**3**), Er (**4**), Yb (**5**).

Table S1. Crystallographic data for compounds **1-5**.

Parameter	**1**	**2**	**3**	**4**	**5**
Formula	$C_{12}H_{14}N_4O_4Pd$	$C_{62}H_{62}N_{26}O_{32}Pd_5Dy_2$	$C_{62}H_{62}N_{26}O_{32}Pd_5Gd_2$	$C_{62}H_{62}N_{26}O_{32}Pd_5Er_2$	$C_{62}H_{62}N_{26}O_{32}Pd_5Yb_2$
F_w / g mol^{-1}	384.67	2540.37	2529.87	2549.89	2561.45
Crystal system	Monoclinic	Triclinic	Triclinic	Triclinic	Triclinic
Space group	$P2_1/a$	P-1	P-1	P-1	P-1
a / Å	4.5772(2)	12.1673(2)	12.1672(7)	12.1819(6)	12.1945(11)
b / Å	18.3853(10)	12.7713(2)	12.7842(5)	12.7650(5)	12.7509(12)
c / Å	8.1572(4)	13.0477(2)	13.0950(7)	13.0467(6)	13.0041(14)
α / °	90	91.807(1)	91.639(1)	91.676(1)	91.610(3)
β / °	95.268(2)	96.213(1)	96.348(1)	96.338(1)	96.362(3)
γ / °	90	98.618(1)	98.546(1)	98.823(1)	98.873(3)
V / Å^3	683.55(6)	1990.49(5)	1999.83(18)	1990.32(16)	1983.4(3)
Z	2	1	1	1	1
T / K	160(2)	160(2)	160(2)	160(2)	160(2)
Radiation / μ (mm^{-1})	MoKα/ 1.380	MoKα/ 3.060	MoKα/ 2.835	MoKα/ 3.291	MoKα/ 3.544
ρ_{calcd} /g cm^{-3}	1.869	2.119	2.101	2.127	2.144
Reflections collected/unique (R_{int})	10715/1551 (0.0343)	45752/8668 (0.0196)	31987/8633 (0.0736)	36544/8656 (0.0637)	21947/5154 (0.0897)
Reflections with $I>2\sigma(I)$	1137	8109	6372	6793	3749
No. of parameters	197	810	825	811	782
R_1 [$I>2\sigma(I)$], wR_2 [$I>2\sigma(I)$][a,b]	0.0206, 0.0453	0.0231, 0.0496	0.0489, 0.1019	0.0410, 0.0899	0.0539, 0.1227
R_1 (all data), wR_2 (all data)[a,b]	0.0334, 0.0492	0.0256, 0.0502	0.0713, 0.1114	0.0568, 0.0976	0.0766, 0.1375
$(\Delta/\sigma)_{max}$	0.026	0.024	0.027	0.014	0.007
$\Delta\rho_{max}/\Delta\rho_{min}$ (e Å^{-3})	0.68/-0.30	1.42/-0.67	1.72/-1.06	1.71/-1.17	1.42/-1.45
CCDC number	2385399	2385400	2385401	2385402	2385403

[a] $w = 1 / [\sigma^2(F_o^2) + (aP)^2 + bP]$, where $P = [\max(F_o^2, 0) + 2F_c^2] / 3$; a = 0.0258, b = 0.1879 for **1**; a = 0.0173, b = 2.7355 for **2**; a = 0.0400, b = 4.7272 for **3**; a = 0.0388, b = 4.0253 for **4**; a = 0.0597, b = 6.5554 for **5**; [b] $R_1 = \Sigma(|F_o| - |F_o|) / \Sigma(|F_o|)$ and $wR_2 = \{\Sigma[w(F_o^2 - F_c^2)^2] / \Sigma[w(F_o^2)^2]\}^{1/2}$.

Table S2. Selected bond distances (Å) and bond angles (º) for complex **1**.

Bond Distances (Å)			
Pd-N1A	2.039(4)	Pd-N2A	2.060(9)
Pd-N1A'	2.039(4)	Pd-N2A'	2.060(9)
Bond Angles (º)			
N2A-Pd-N1A	80.2(2)	N2A'-Pd-N1A'	80.2(2)
N2A-Pd-N1A'	99.8(2)	N1A-Pd-N1A'	180.0
N2A'-Pd-N1A	99.8(2)	N2A-Pd-N2A'	180.0

Symmetry code: (') *-x*, *2-y*, *2-z*.

Table S3. Selected bond distances (Å) and bond angles (º) for complex **2**.

Bond Distances (Å)			
Pd1-N1A	2.042(3)	Dy1-O2	2.469(3)
Pd1-N1A'	2.042(3)	Dy1-O3	2.449(3)
Pd1-N2A	2.038(5)	Dy1-O5	2.487(2)
Pd1-N2A'	2.038(5)	Dy1-O6	2.457(2)
Dy1-O1A	2.29(3)	Dy1-O8	2.433(2)
Dy1-O1W	2.286(2)	Dy1-O9	2.519(2)
Dy1-O1M	2.340(2)		
Bond Angles (º)			
N2A-Pd1-N1A	78.95(17)	O6-Dy1-O5	51.40(8)
N2A-Pd1-N1A'	101.05(17)	O6-Dy1-O9	121.28(8)
N2A'-Pd1-N1A	101.05(17)	O8-Dy1-O2	143.75(10)
N2A'-Pd1-N1A'	78.95(17)	O8-Dy1-O3	141.94(9)
N1A-Pd1-N1A'	180.0	O8-Dy1-O5	69.49(8)
N2A-Pd1-N2A'	180.0	O8-Dy1-O6	74.41(8)
O1A-Dy1-O2	80.3(5)	O8-Dy1-O9	51.13(7)
O1A-Dy1-O3	87.4(7)	O1M-Dy1-O2	75.88(11)
O1A-Dy1-O5	148.7(8)	O1M-Dy1-O3	127.39(10)

O1A-Dy1-O6	152.6(6)	O1M-Dy1-O5	125.25(8)
O1A-Dy1-O8	124.4(6)	O1M-Dy1-O6	77.64(8)
O1A-Dy1-O9	73.3(6)	O1M-Dy1-O8	79.74(10)
O1A-Dy1-O1M	86.0(8)	O1M-Dy1-O9	73.21(9)
O2-Dy1-O5	103.95(9)	O1W-Dy1-O1A	77.0(7)
O2-Dy1-O9	140.29(9)	O1W-Dy1-O2	123.57(10)
O3-Dy1-O2	51.57(10)	O1W-Dy1-O3	76.29(9)
O3-Dy1-O5	72.67(9)	O1W-Dy1-O5	75.01(8)
O3-Dy1-O6	85.34(9)	O1W-Dy1-O6	126.38(8)
O3-Dy1-O9	151.35(9)	O1W-Dy1-O8	90.10(9)
O5-Dy1-O9	114.07(8)	O1W-Dy1-O9	78.82(8)
O6-Dy1-O2	74.45(9)	O1W-Dy1-O1M	150.47(9)

Symmetry code: (') -*x*, -*y*, 1-*z*.

Table S4. Continuous Shape Measurement (CShM) values for the potential coordination polyhedra of the 9-coordinate Dy1/Dy1' centers in complex **2**.

Polyhedron[a,b]	**Dy1/Dy1'**
EP	34.64
OPY	21.86
HBPY	16.58
JTC	14.43
JCCU	9.62
CCU	8.19
JCSAPR	3.35
CSAPR	2.57
JTCTPR	3.60
TCTPR	2.82
JTDIC	12.03
HH	8.99
MFF	**2.43**

[a]Abbreviations: EP, Enneagon; OPY, Octagonal pyramid; HBPY, Heptagonal bipyramid; JTC, Johnson triangular cupola; JCCU, Capped cube; CCU, Spherical-relaxed capped cube; JCSAPR, Capped square antiprism, CSAPR-9, Spherical capped square antiprism; JTCTPR, Tricapped trigonal prism; TCTPR, Spherical tricapped

trigonal prism; JTDIC, Tridiminished icosahedron, HH, Hula-hoop; MFF, Muffin. [b]The value in boldface indicates the closest polyhedron according to Continuous Shape Measures.

Table S5. Hydrogen bonding interactions in the crystal structure of **1**·2H$_2$O. Abbreviations: D = Donor; A = Acceptor

D—H···*A*	*D*—H (Å)	H···*A* (Å)	*D*···*A* (Å)	*D*—H···*A* (°)
Intramolecular				
C6*A*—H6*A*···O1*A*^{i}	0.95	2.15	2.947(10)	140
C6*B*—H6*B*···O1*B*^{i}	0.95	2.13	2.924(16)	141
Intermolecular				
C5*A*—H5*A*···O1*A*^{ii}	0.95	2.86(1)	3.343(12)	113(1)
C1*B*—H1*B*···O1*B*^{iii}	0.95	2.44(1)	3.194(2)	136.1(5)
*O1*W*—H1*WA*···O1*A*^{iv}	0.80(5)	2.01(4)	2.80(3)	170(4)
*O1*W*—H1*WA*···O1*B*^{v}	0.80(5)	2.01(4)	2.79(3)	166(4)
*O1*W*—H1*WB*···O1*W*^{vi}	0.74(5)	1.98(5)	2.69(4)	163(5)

*Only the parameters for water molecules occupying sites A are given.

Symmetry codes: (i) -*x*, -*y*+2, -*z*+2; (ii) *x*, *y*, *z*-1; (iii) -*x*, -*y*+2, -*z*+1; (iv) *x*+1, *y*, *z*-1; (v) -*x*+1, -*y*+2, -*z*+1; (vi) *x*+1/2, -*y*+3/2, *z*.

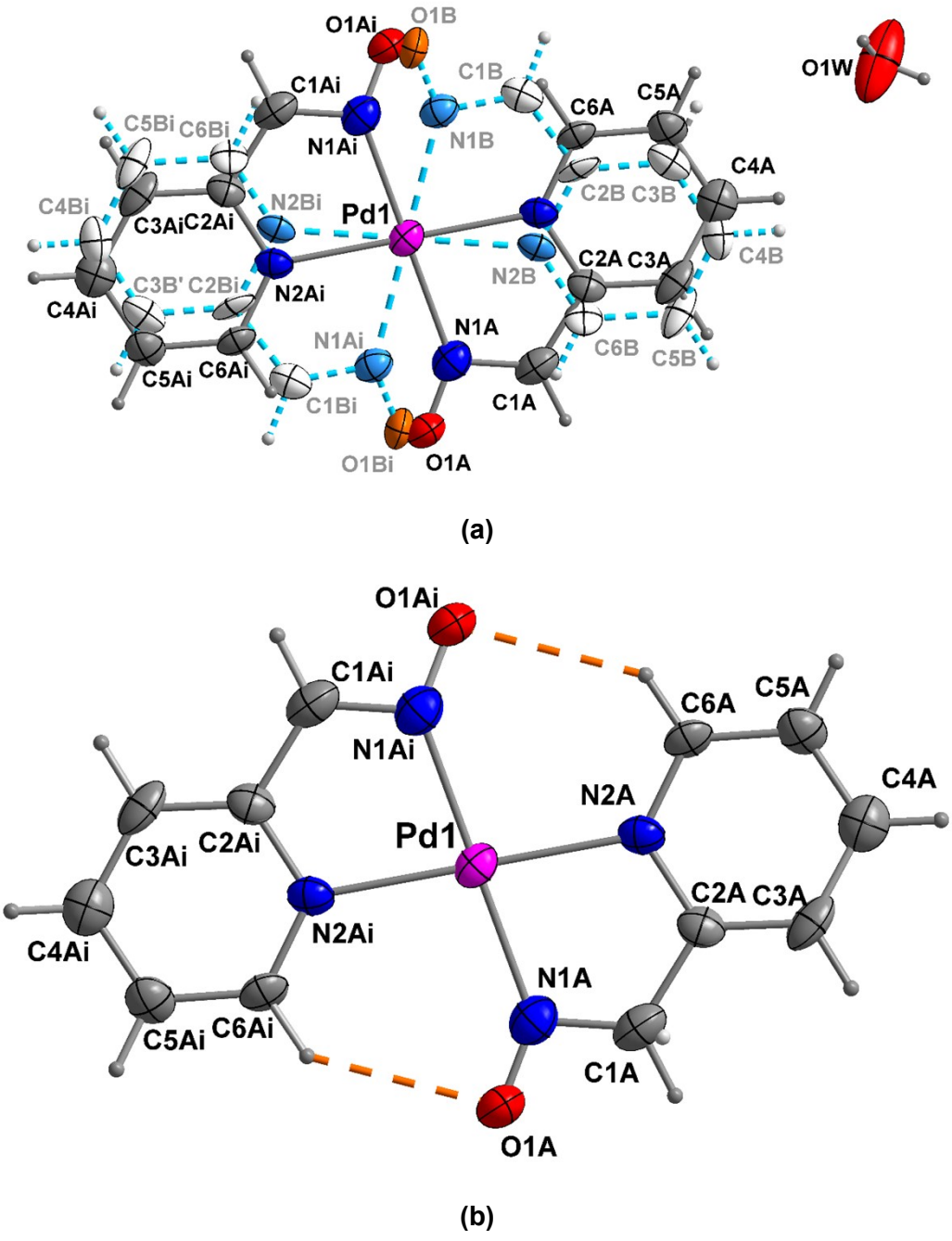

Figure S3. (a) Fully labelled ORTEP plot of **1**·2H₂O. Atoms labeled as "A" and "B" indicate the two disordered orientations of the ligands. Dashed cyan lines connect the atoms in orientation B. The atoms occupying sites B are decorated with lighter colors. (b) Fully labelled ORTEP plot of **1** using the disordered orientation which corresponds to A atoms; the dashed orange lines highlight the C6A—H6A···O1A' intramolecular hydrogen bonds. Color scheme: Pd^{II}, magenta; O, red; N, blue; C, gray. Symmetry code: (i): *-x*, 2-*y*, 2-*z*.

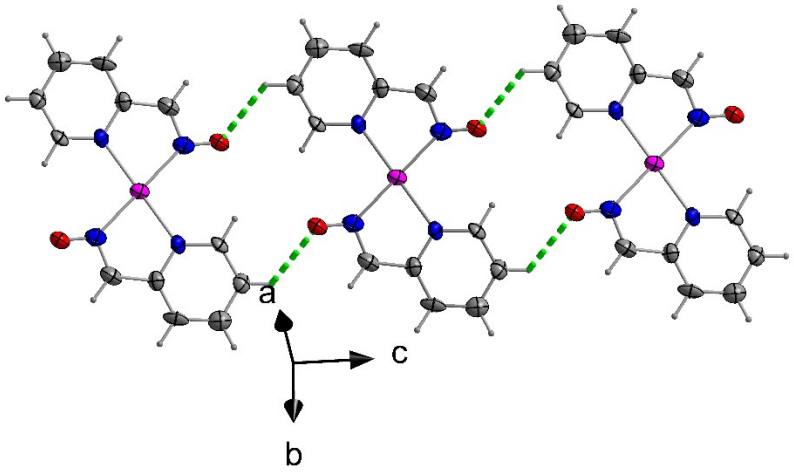

(a)

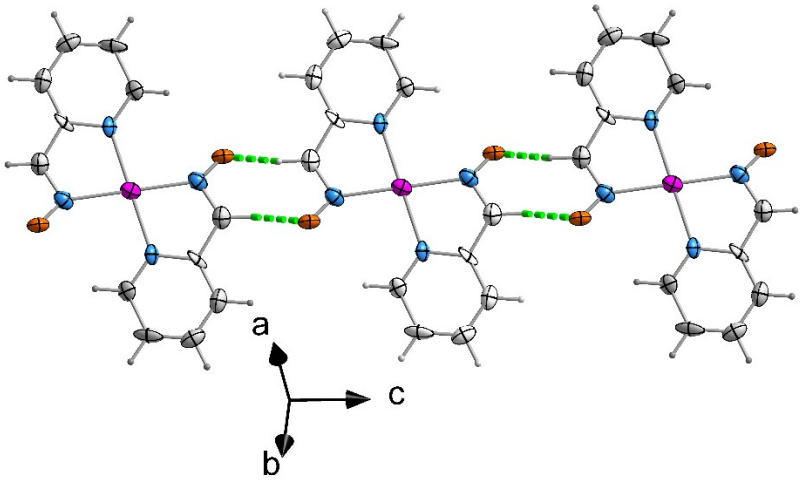

(b)

Figure S4. Intermolecular hydrogen bonds between the two disordered parts of the [Pd(pao)$_2$] complexes in the structure of **1**. In (a), the hydrogen bonds developed among the A disordered parts and in (b) those developed among parts B are shown, i.e. C5*A*-H5*A*···O1A^{ii} and C1B-H1B···O1B^{iii} (symmetry codes are given in Table S5 or in the text). Color coding is as in Figure S3.

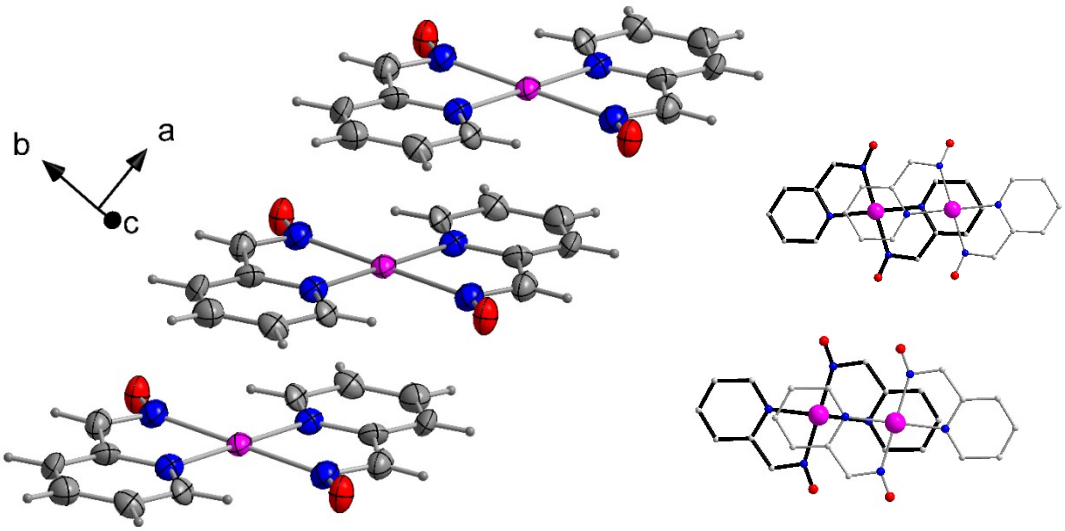

Figure S5. Stacking of [Pd(pao)$_2$] complexes with the pao$^-$ ligands in A-orientation. In the inset, the overlap type of neighboring complexes is shown for A-orientation (top) and B-orientation (bottom). Those at the top are with light colors. Color coding as in Figure S3.

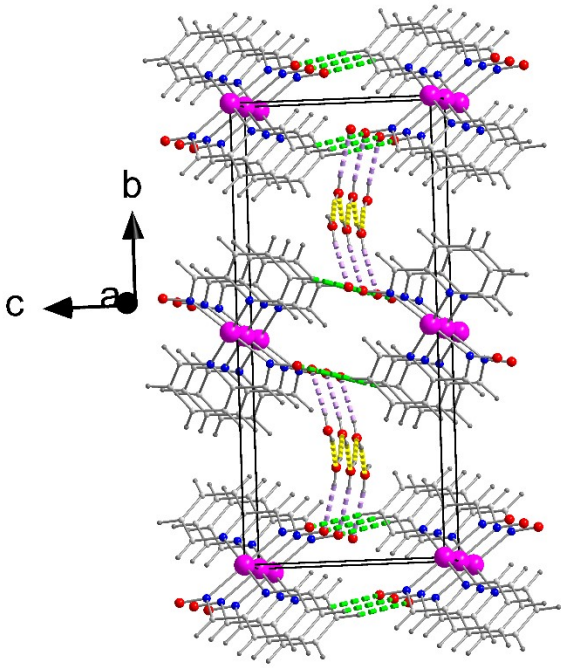

Figure S6. 3-D architecture of the structure of **1**·2H$_2$O. The pao$^-$ ligands and water lattice solvent molecules are presented only occupying site A. Dashed green, yellow and violet lines highlight the C5*A*-H5*A*···O1A^{ii}, O1*WA*-H2W···O1*WA*^{vi} and O1*WA*-

H1*W*···O1*A*^{iv} hydrogen bonding interactions (symmetry codes are given in Table S5). Color coding as in Figure S3.

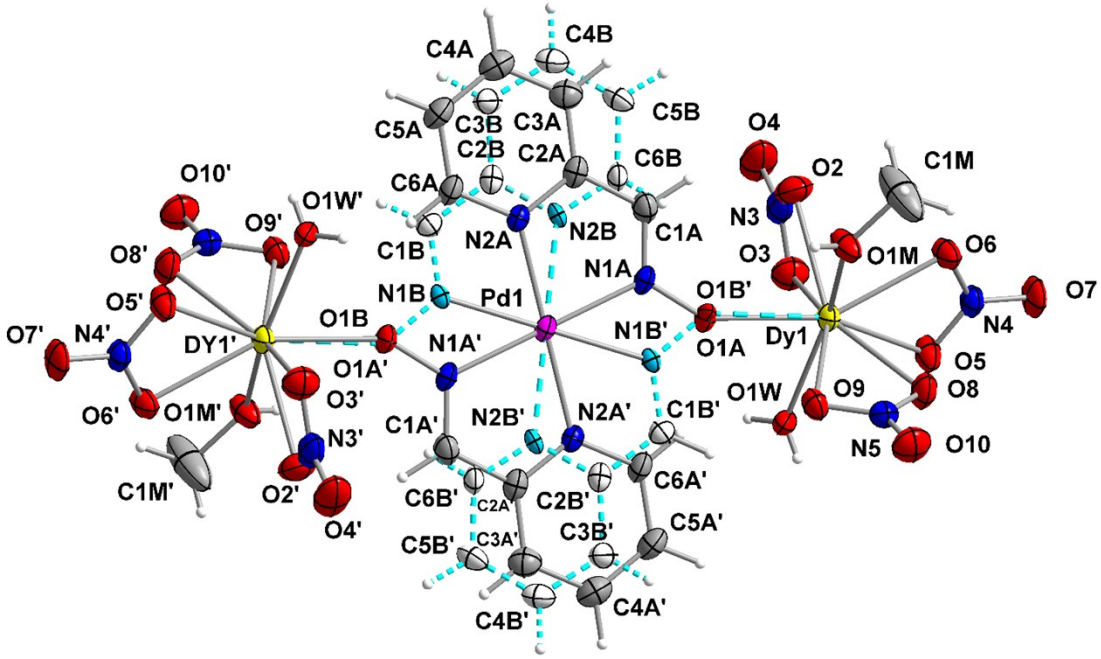

(a)

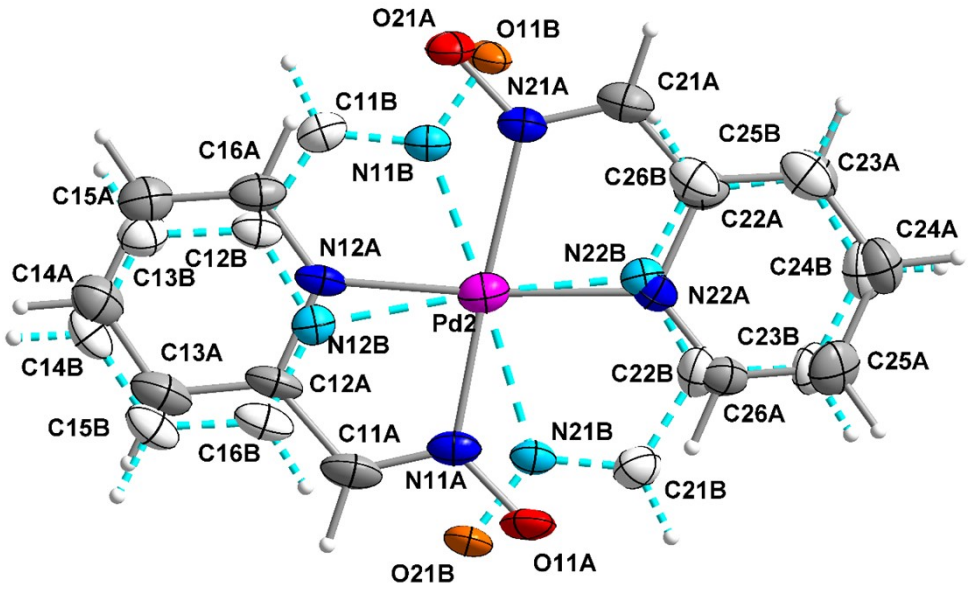

(b)

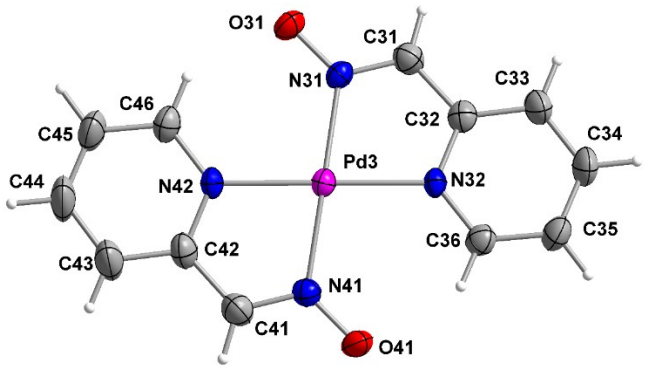

(c)

Figure S7. Ortep-type views of the complexes (a) **2A**, (b) **2B**, and (c) **2C** that are present in the structure of **2**. Atoms labeled as A and B in (a) and (b) indicate the two disordered orientations of the pao$^-$ ligands. Dashed cyan lines connect the atoms in orientation B and the atoms occupying sites A are highlighted with lighter colors. Symmetry code (′): -*x*, -*y*, 1-*z*.

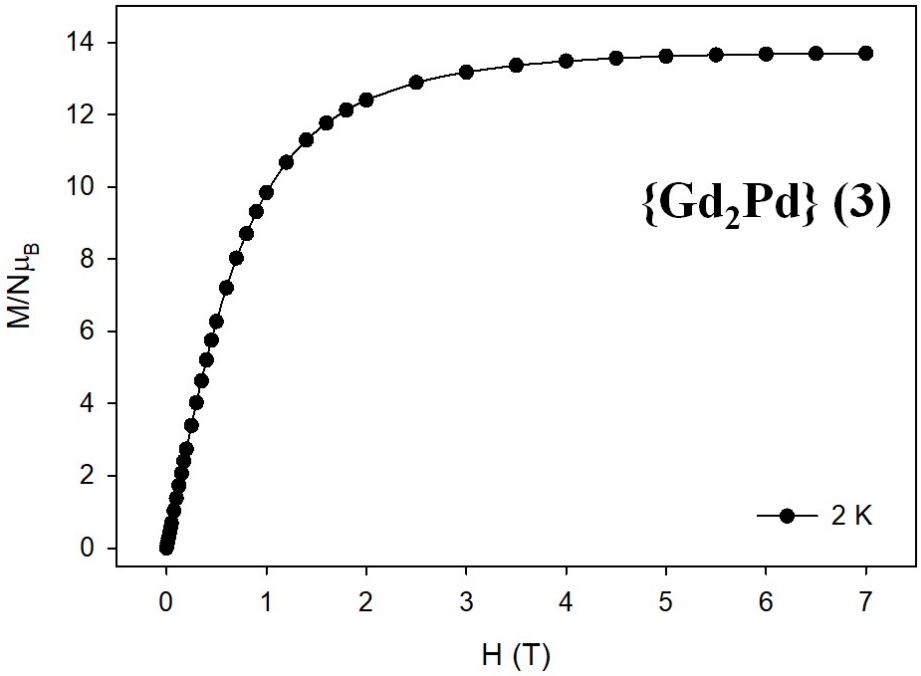

Figure S8. Plot of magnetization (*M*) *vs.* field (*H*) for complex **3** at 2 K. The solid line is guide for the eye only.

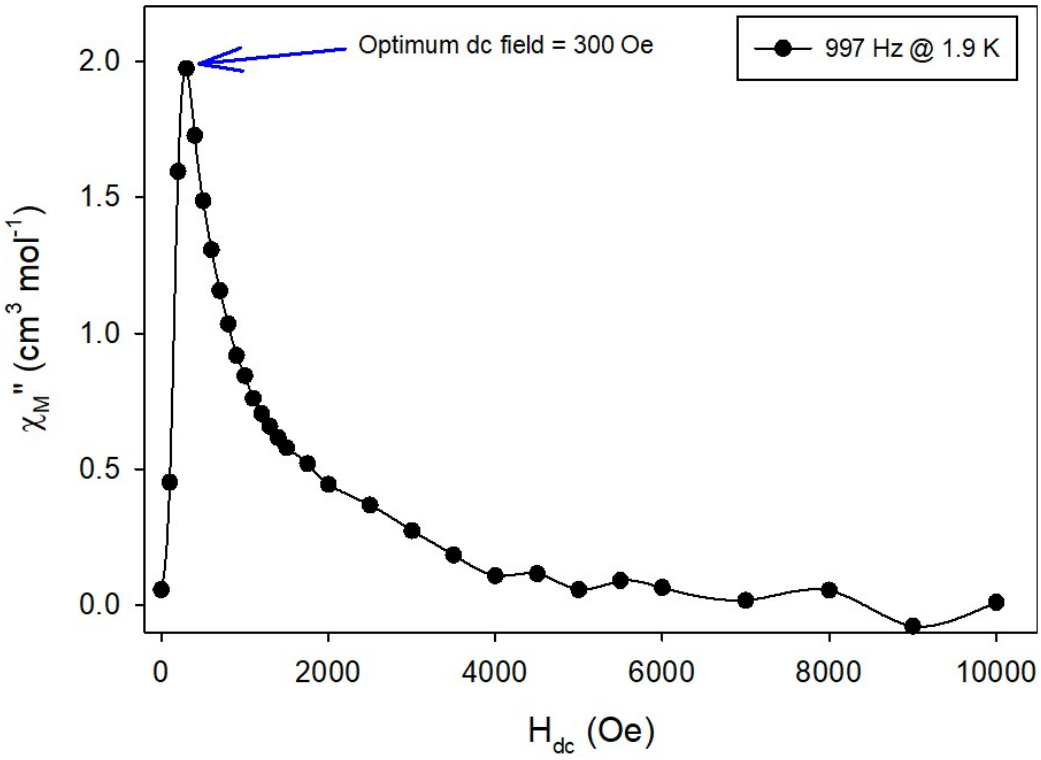

Figure S9. Plot of out-of-phase *ac* magnetic susceptibility (χ''_M) *vs.* field (*H*) for complex **2** at 1.9 K, indicating an optimum *dc* field at 300 Oe.

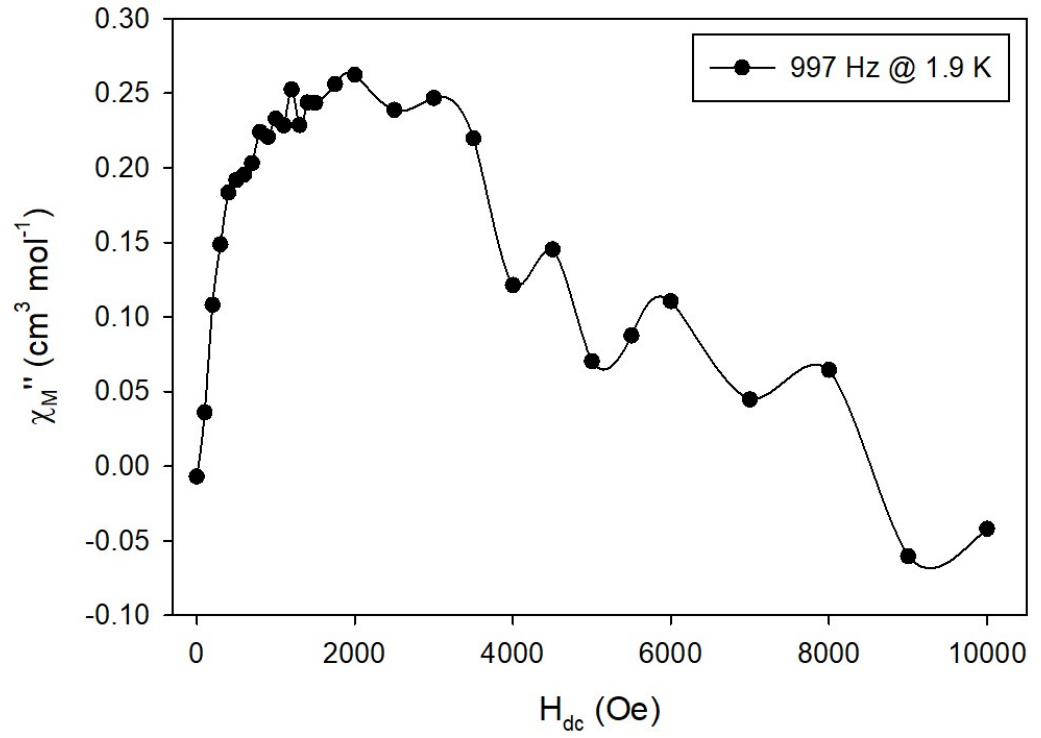

Figure S10. Plot of out-of-phase *ac* magnetic susceptibility (χ''_M) *vs.* field (*H*) for complex **5** at 1.9 K, indicating an optimum *dc* field at 2000 Oe.

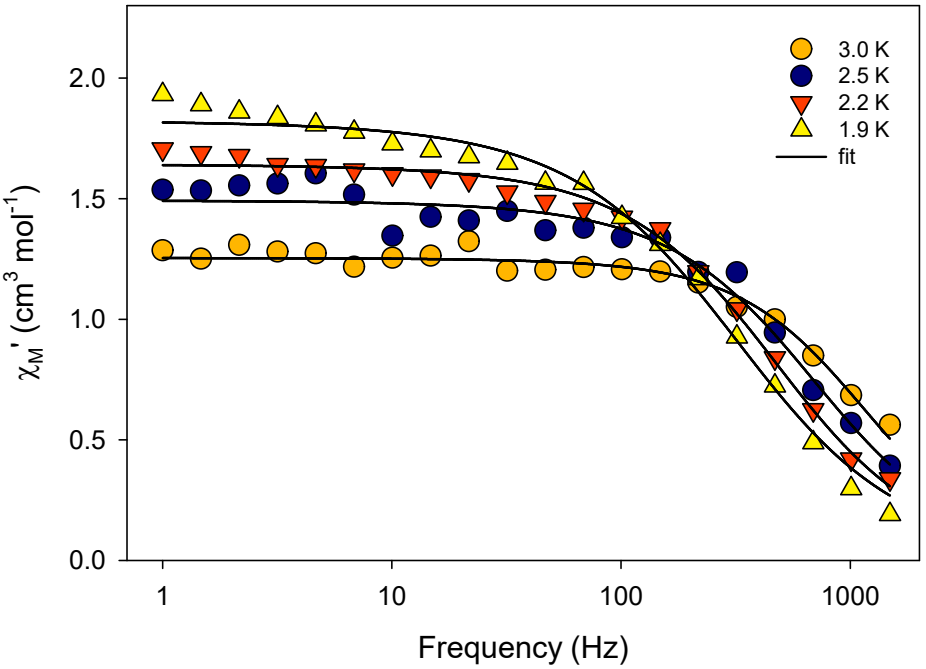

Figure S11. Frequency dependence of the in-phase (χ'_M) *ac* magnetic susceptibility under a 2000 Oe applied optimum *dc* field for complex **5**. Solid lines correspond to the best fit obtained with a generalized Debye model.

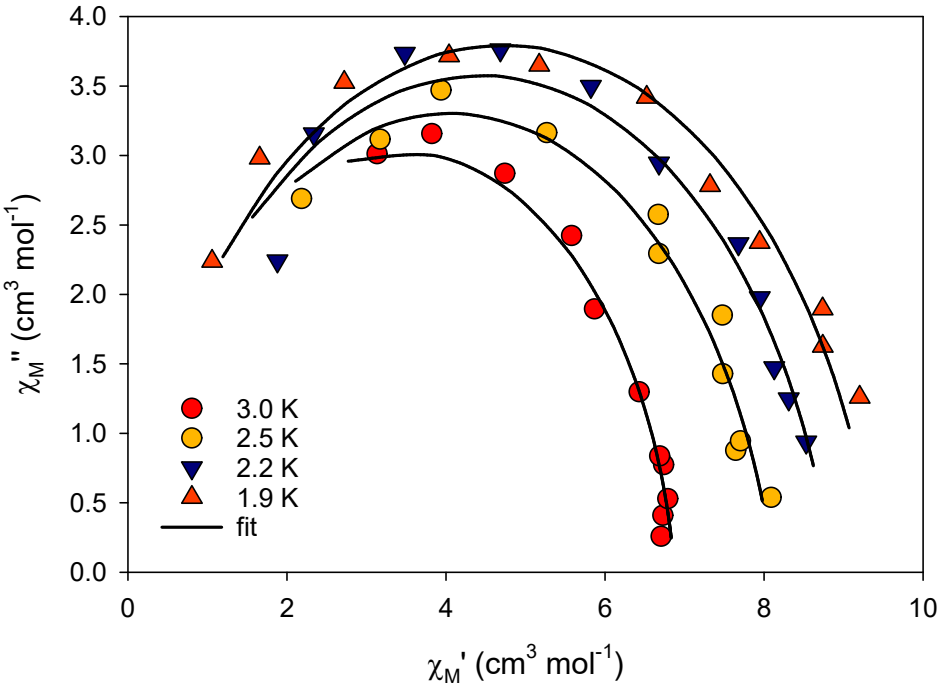

Figure S12. Cole-Cole plot for complex **5** obtained using the *ac* susceptibility data under a 2000 Oe applied *dc* field at the temperature range 1.9-3.0 K. The solid lines correspond to the best fit obtained with a generalized Debye model.